

Supplemental Material

Surface-Enhanced Raman Scattering (SERS) Studies of Disc-on-Pillar (DOP) Arrays: Contrasting Enhancement Factor with Analytical Performance

Raymond A. Velez¹, Nickolay V. Lavrik², Ivan I. Kravchenko², Michael J. Sepaniak³, and Marco A. De Jesus^{1*}

¹University of Puerto Rico, Department of Chemistry, PO Box 9000, Mayaguez, Puerto Rico, 00681-9000, USA

²Oak Ridge National Laboratory, Center for Nanophase Materials Sciences, Oak Ridge, TN, 37831, USA

³University of Tennessee at Knoxville, Department of Chemistry, 552 Buhler Hall, Knoxville, TN, 37996, USA

*Corresponding author email: marco.dejesus@upr.edu

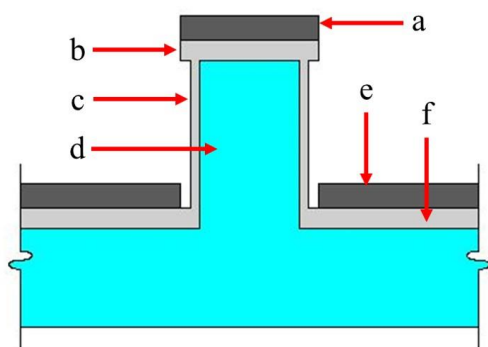


Figure S1. Schematic of DOP structural components used FDTD modelling: (a) Ag disk, $h = 25$ nm, $d = 120$ nm; (b) SiO₂ on pillar top, $h = 20$ nm, $d = 120$ nm; (c) SiO₂ on pillar sidewalls, $h = 155$ nm, $d = 155$ nm, i.d./o.d. = 80 nm/100 nm; (d) Si pillar, $h = 175$ nm, $d = 80$ nm; (e) Ag mirror, $h = 25$ nm, i.d./o.d. = 120 nm/4000 nm; (f) SiO₂ on etched wafer surface, $h = 20$ nm, $d = 1000$ nm. d = diameter, h = height, i.d. = inner diameter, and o.d. = outer diameter.

Disc-on-Pillar (DOP) Fabrication

The general nanofabrication process used a previously cleaned single crystal silicon (SCS <100>) wafer. The nanofabrication recipe consisted of adding about 1 mL of P20 Adhesion Promoter and spin coating at 3000 rpm for 40 seconds. Afterwards, about 1 mL of ZEP 520A was applied and spin coated under the same conditions followed by a soft-bake at 180 °C for

2 min. thus producing the resist film with a final thickness about 250 nm. The substrate pattern was imprinted with a Jeol JX 9300FS electron beam lithography system (EBL) using a $400 \mu\text{C}/\text{cm}^2$ dose. The total EBL process was completed in about 40 min. Pattern development was accomplished by submerging the wafer for 40s in Xylene, then another 40s in isopropyl alcohol (IPA), followed by a final IPA rinse and N_2 drying. The pattern was randomly checked (using a Nikon Eclipse LV100 optical microscope (20x and 50x)). A 15 s substrate descumming was performed within an oxygen plasma system (PVA TePla Ion Wave 10). A 100 \AA Cr mask was deposited under vacuum (4.7×10^{-6} torr), with a VE-240 dual electron gun evaporator at a rate of $1 \text{ \AA}/\text{second}$. Lift-off process was achieved by submerging the wafer in an acetone bath for 60s, followed by a second 30 s clean on a fresh acetone batch. The cleaned surface was then rinsed with IPA and DIW. Si pillar arrays were rendered with a Plasma Lab System 100 Reactive Ion Etcher with a mixture of $\text{Ar}/\text{C}_4\text{F}_8/\text{SF}_6$. After descumming, the etched substrate for 1 min., the Cr mask was chemically removed by submerging substrates in CR14S for 2 min. followed by 30 seconds of IDW. A thin, conformal layer (20 nm) of SiO_2 was deposited on the pillars using an Oxford ALD (202 cycles at $0.99 \text{ \AA}/\text{cycle}$ at 300°C). Refer to Figures S1 and S2 for a schematic of the DOP structure components and the fabrication process.

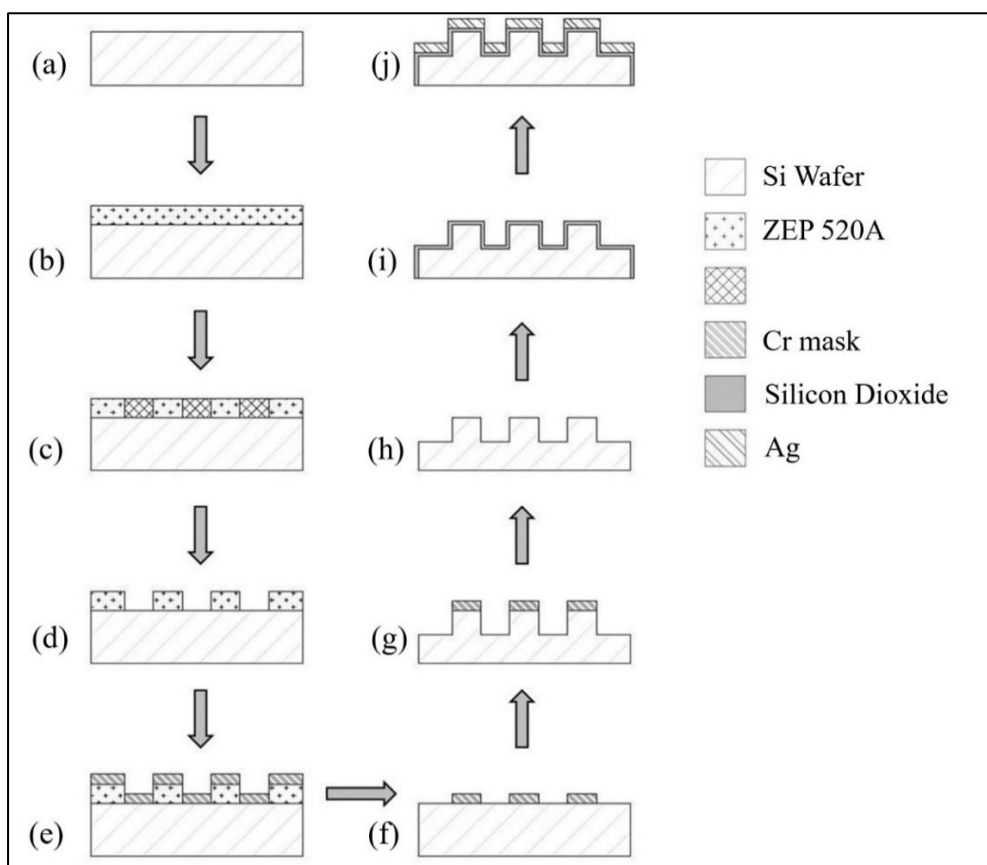


Figure S2. General fabrication summary of DOP periodic arrays (Drawings are not to scale). (a) Previously cleaned Si wafer; (b) addition of ZEP520A photoresist; (c) EBL-imprinting pattern; (d) development and descumming; (e) application of Cr mask; (f) substrate after Lift-off; (g) etched Si wafer; (h) after Cr stripping; (i) SiO₂ layer growth; (j) metallization via PVD.

Calibration Sensitivity

Calibration sensitivity was assessed by constructing calibration curves for R6G (10^{-6} M to 10^{-3} M). A 20 μ L drop was placed on the chip and covered with a microscope coverslip.

Replicate Raman spectra for the periodicities of interest were obtained immediately.

Afterwards, the chip was washed with copious amounts of DIW, EtOH, and a final rinse of DIW followed by air drying. Spectra for R6G standards were obtained in a random order. A blank spectrum of the chip was acquired prior to obtaining an R6G reading to confirm the absence of interferences from the previous sample. R6G was not considered for determination of EF because the SERS response would be a result of plasmonic, chemical, and resonant enhancements, thus interfering with the determination of the LSP (electromagnetic) contribution to the EF. However, R6G resulted attractive to assess

sensitivity in order to determine the breadth of the detection range for a SERS platform with an optimized plasmonic response. Spectra of 4-ABA samples at concentrations of 10^{-4} M and 10^{-5} M were obtained for pillar arrays of interest to further elucidate the performance of the optimized DOP system with an analyte of moderate physisorption onto the SERS surface.

BT SAM Temporal Study

This study was executed to assess the adequacy of the BT incubation time reported.

A water bath was prepared on top of a magnetic stirring plate using a shallow tray and an automatic temperature controlled recirculator (Thermo Scientific, Arctic S150-A10). Approximately 7.5 mL of ethanolic BT solutions with a final concentration of 1×10^{-3} M and 1×10^{-5} M added to individual petri dishes and equilibrated to 26.5 °C. Individual chips were incubated for 15 min. in approximately with constant stirring. A glass-coated magnetic stir bar (Cole-Palmer Item EW-04769-50) was used to minimize adsorption of BT molecules to surfaces other than the chip. Afterwards the chip was dipped in DIW followed by rinsing with copious amounts of DIW and drying with N₂. Raman spectra were obtained in duplicate of p160 and p520. The chips were returned to their original solutions and incubated for a total of 1200 min. (20 hours). The DIW rinse and drying process was repeated and additional spectra obtained for p160 and p520.

Spectra were obtained using a JY-Horiba LabRAM HR800 Raman microscope equipped with a HeNe laser ($\lambda = 632.81$ nm, power = 7.50 mW) and a long working distance 50x objective (NA = 0.45 μ m, effective spot size = 2.0 μ m). Individual spectra were measured with 1 second acquisition time. A 600 nm grating, 400 μ m aperture and 200 μ m slit width were used in all SERS measurements. The spectral range was from 200 cm^{-1} to 4000 cm^{-1} . All spectra were baseline corrected and background subtracted.

The spectra (Figure S3) do not depict significant differences in band response between 10^{-5} M and 10^{-3} M at each incubation interval for p160 and p520. There was a slight redshift from 1074 cm^{-1} to 1072 cm^{-1} for samples corresponding to the incubation period of 1200 min. The 2 cm^{-1} represents roughly a -0.2% difference in Raman shift. Any difference less than 5 cm^{-1} is not considered a significant.

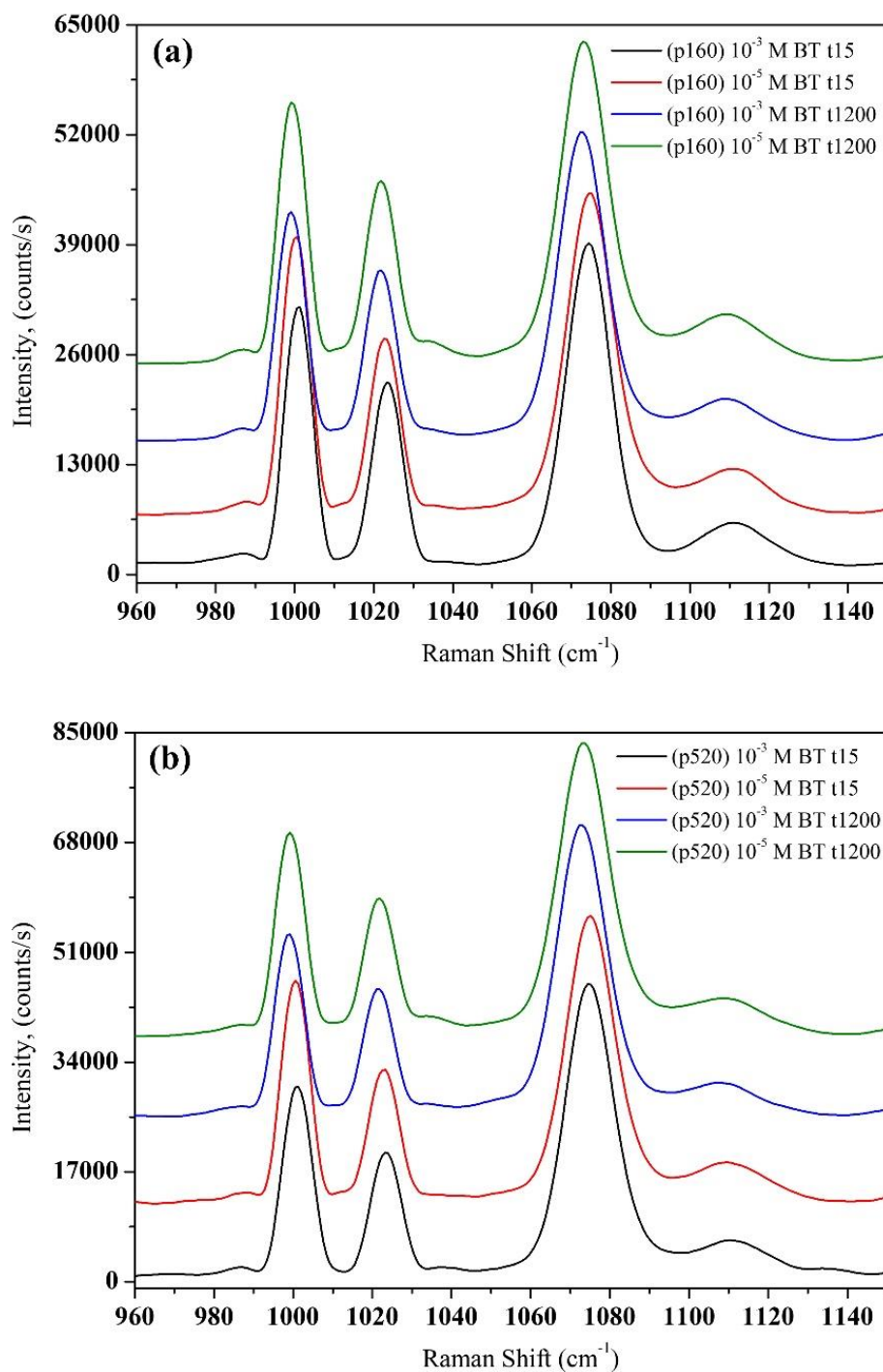


Figure S3: Mean SERS spectra for 1.0×10^{-3} M and 1.0×10^{-5} BT using the $24 \mu\text{m} \times 24 \mu\text{m}$ DOP region for (a) p160 and (b) p520. All spectra are offset in the y-axis for clarity. A slight red shift ($< 2 \text{ cm}^{-1}$) is observed for samples corresponding to the 1200 incubation period. This shift is a -0.2% difference and is not considered significant.

The relative difference between sample intensities as per the following equation:

$$\text{Relative Intensity Difference} = \left(\frac{I_{t1200} - I_{t15}}{I_{t15}} \right) \times 100$$

where I_{t15} and I_{t1200} correspond to the C–S band intensity for the incubation times at 15 and 1200 min. respectively.

Table S1 depicts the differences calculated for the different sample iterations. The following can be established from the results:

- The relative differences between incubation periods of 15 and 1200 min. are not considered significant ($< 1.5\%$). The greatest difference is observed for the higher concentration (1×10^{-3} M) although considered insignificant.
- The relative differences between concentrations within the same incubation time for each pitch is not considered significant ($< 1\%$).

Table S1. C–S band intensity (counts/s) of 10^{-3} M and 10^{-5} M BT at incubation periods of 15 min. and 1200 min. using p160 and p520 DOP plasmonic systems.

DOP	[BT] M	Intensity (counts/s)		% Relative difference		
		t15	t1200	t15 versus t1200	10^{-3} M versus 10^{-5} M (t15)	10^{-3} M versus 10^{-5} M (t1200)
p160	1×10^{-3}	38491.3	38051.3	–1.1	–0.5	0.2
p160	1×10^{-5}	38313.4	38134.5	–0.5		
p520	1×10^{-3}	45948.9	45238.6	–1.5	–0.5	0.2
p520	1×10^{-5}	45250.3	45544.0	0.6		

In summary, the data did not show significant differences between incubation times and BT concentration used. This suggests that the conditions reported to render a BT layer on the DOP system, which are 15 min. incubation time with a 1×10^{-5} M, are considered adequate for SSEF assessment. Moreover, the data is consistent with reported low ΔG_{ads} (-7.40 kcal/mol, -8.8 kcal/mol) as well as with fast thiol adsorption kinetics.^{1–3}

Maximum Allowable Pillars (MAP)

The number of pillars within the spot is accounted for by the value of MAP, which is based on the laser spot area (A_L) and the area occupied by one pillar (A_P) as per the array pitch (Eqs. 3 to 5). The beam waist of the laser is presumed to have a circular shape based on the optical imaging. A schematic representation of MAP is shown (Figure S4).

$$A_P = \frac{\text{pillar}}{\text{pitch}^2} \quad (\text{S1})$$

$$A_L = \pi r_L^2, \text{ where } r_L \text{ is the laser spot radius} \quad (\text{S2})$$

$$\text{MAP} = A_P \times A_L = \frac{\text{pillar} \times \pi r_L^2}{\text{pitch}^2} \quad (\text{S3})$$

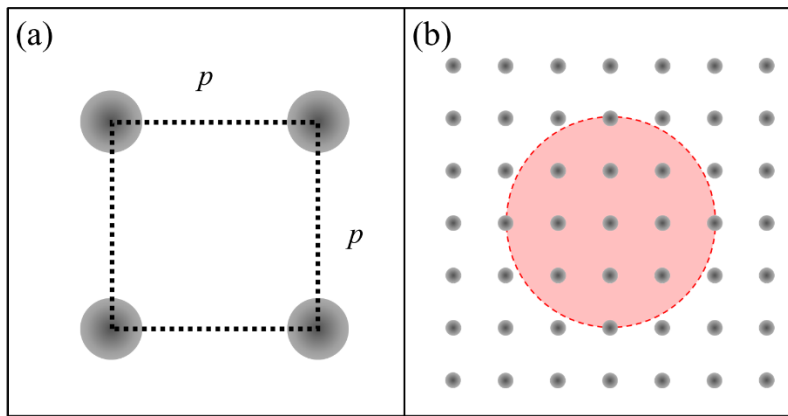


Figure S4. Schematic representation (not to scale) of the maximum allowable pillar (MAP). (a) The area occupied by one DOP, A_P . (b) The laser beam spot, A_L , (represented by the red circle) confining an array of disc-on-pillars (DOP).

The MAP equation does not account for pillar-to-pillar variability such as differences in pillar dimensions or inconsistent gaps, hence the importance of inspecting the fabricated substrates with high resolution techniques such as scanning electron microscopy (SEM). Any imperfections that are not detectable in the micrographs is considered insignificant.

MAP plays a significant role for the DOP systems studied because it normalizes the SERS response for all periodicities thus allowing for a rational comparison between pillar arrays of different pitch values. For instance, a 50x objective with a 2 μm beam spot diameter will have an estimate MAP of 123 pillars for a 160 nm pitch (denoted as p160) and 12 pillars for 520 nm pitch (denoted as p520). Considering a 4x4 array, the 16 pillars corresponding to

p160 will be located within the beam spot whereas only 12 of the 16 pillars will fit for the p520. However, a 2×2 array will accommodate all pillars within the laser spot regardless of the inter-pillar spacing, thus allowing a direct assertion of the SERS activity for all arrays because all parameters, except for the pitch, are kept constant. Under the current instrumentation conditions, normalization with MAP is required for the periodicities studied with DOP arrangements greater than 2×2 .

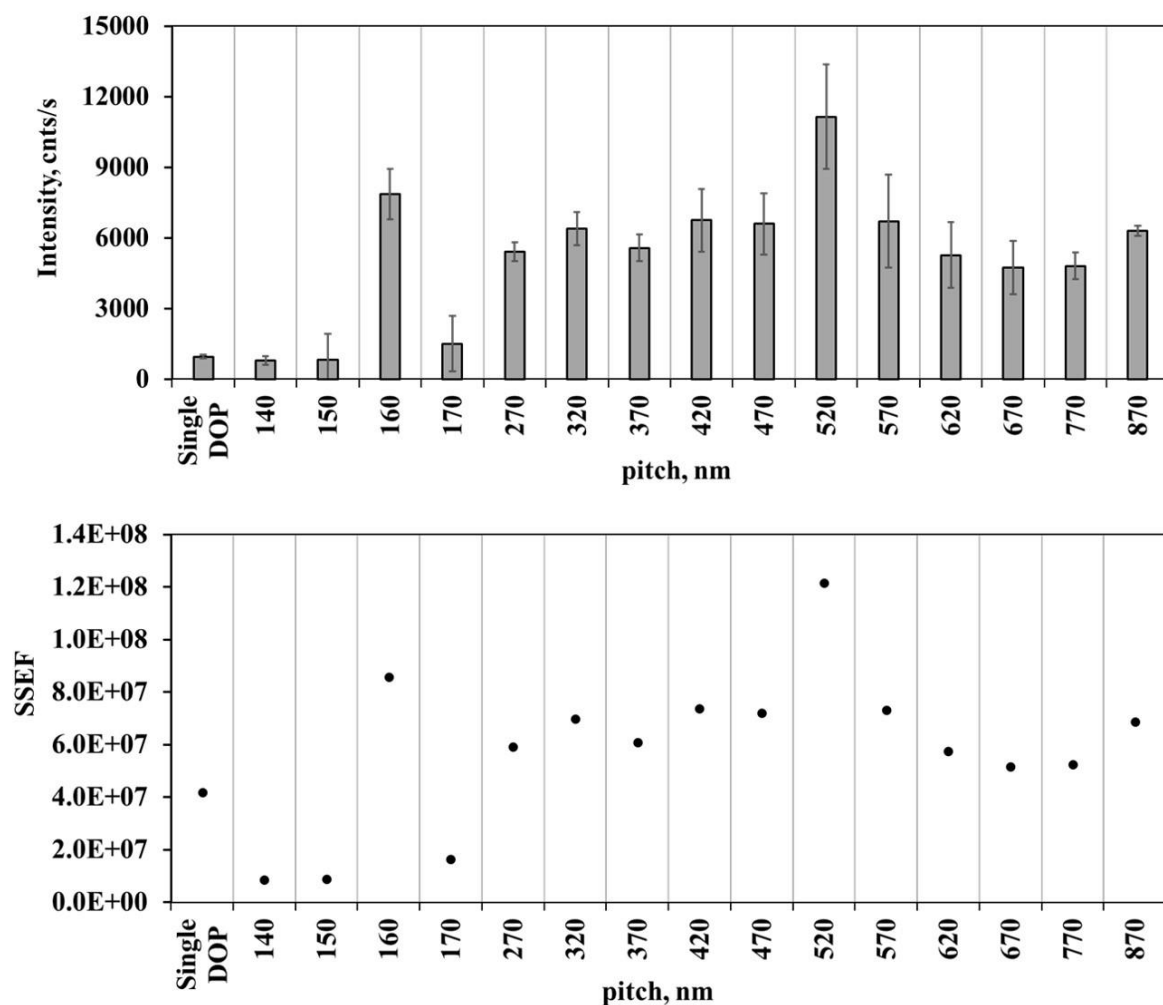


Figure S5. (Top) BT SERS response for 2×2 DOP arrays and a single pillar. The total number of pillars probed ($n = 4$) was the same for all periodicities. The error bars are the standard deviation of triplicate measurements made around the center of the array. The CV calculated for each pitch ranged from 4.0% to 8.9%. (Bottom) Calculated SSEF for single pillar and periodic arrays. An excellent correlation ($R^2 = 1.000$) was obtained for SSEF and SERS raw signal.

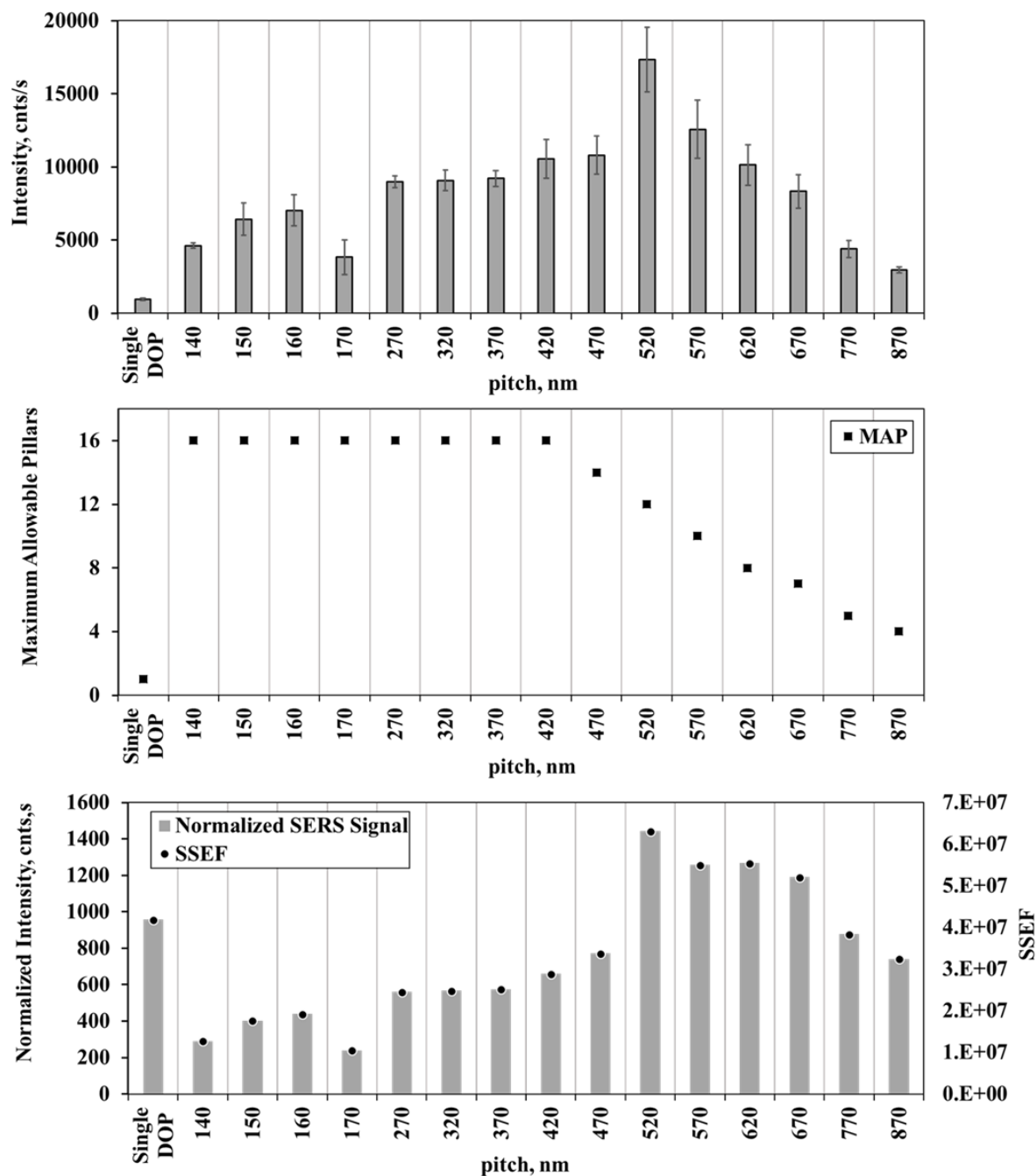


Figure S6. BT SERS activity using 4×4 DOP arrays. The error bars are the standard deviation of triplicate measurements made around the center of the array. The calculated CV for each period ranged from 3.1% to 9.2%. The area for 1075 cm^{-1} ($\nu_{\text{C-S}}$) was normalized with the MAP of each pitch for a $2 \mu\text{m}$ laser spot.

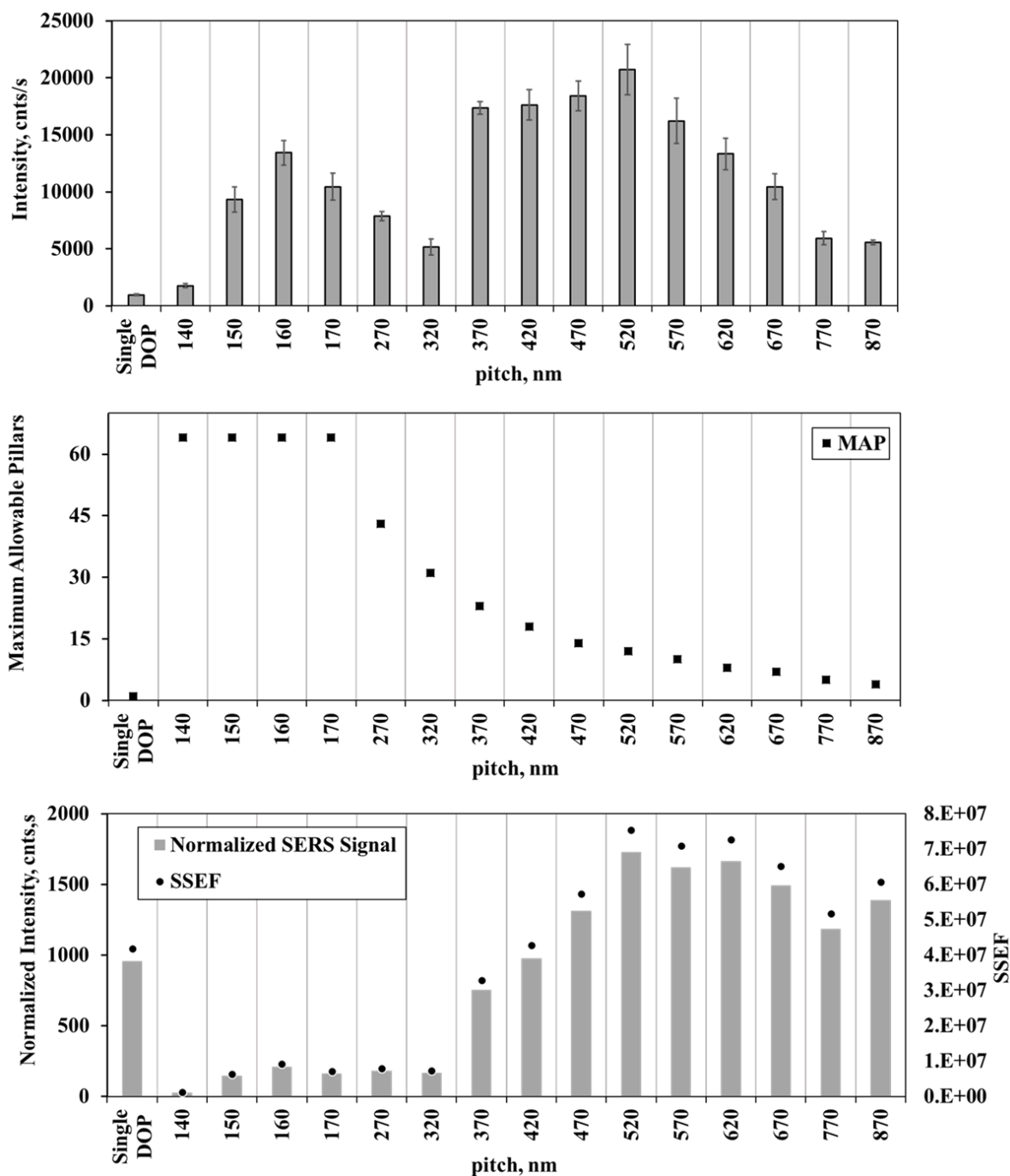


Figure S7. BT SERS activity using 8×8 DOP arrays. The error bars are the standard deviation of triplicate measurements made around the center of the array. The calculated CV for each period ranged from 2.6% to 9.6%. The area for 1075 cm^{-1} ($\nu_{\text{C-S}}$) was normalized with the MAP of each pitch for a $2 \mu\text{m}$ laser spot.

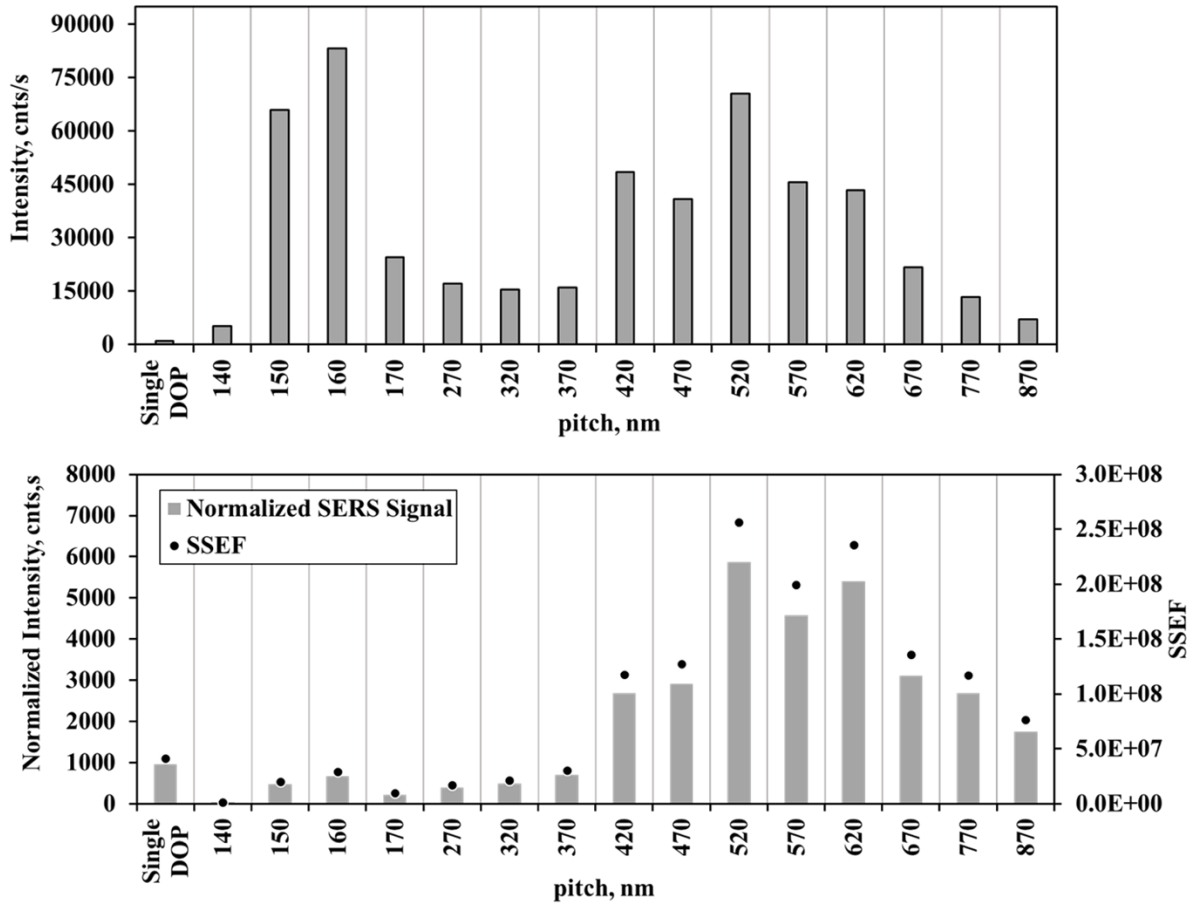


Figure S8. (top) Average BT SERS response for the full $24 \times 24 \mu\text{m}$ array region as determined by LabSpec Software. (bottom) BT SERS response after normalization with MAP and calculated SSEF.

DOP Pitch Order Response Factor

The DOP pitch order response factor (Φ) between two arrays of the 520 nm pitch was calculated with the non-normalized SERS response of the BT 1075 cm^{-1} band using the following equation:

$$\Phi_{2,1} = \left(\frac{\text{SERS}_2}{\text{SERS}_1} \right) \quad (\text{S4})$$

where SERS_1 and SERS_2 correspond to SERS response of two different arrays the latter being the higher order array system (as per responses depicted in Table S2).

Table S2. SERS response of the BT 1075 cm^{-1} for various arrays of the 520 nm pitch and of the single pillar.

Pillar	BT 1075 cm ⁻¹
arrangement	Intensity (counts/s)
Single DOP	956.67
2 × 2	11148.07
4 × 4	17331.30
8 × 8	20729.80
24 μm ²	87412.20

Consider the performance of 2 × 2 and 8 × 8 pillar arrays. Using the BT band response provided in Table S2 renders a stronger SERS response for the 8 × 8 over 2 × 2 by a factor of 1.9. The calculations are as follows:

$$\Phi_{2,1} = \left(\frac{20729.80 \text{ counts/s}}{11148.07 \text{ counts/s}} \right) = 1.9$$

Table S3 contrasts the SERS performance between different pillar arrays as well as the single pillar. For instance, the 2 × 2 pillar array has a 11.7 stronger response than the single pillar whereas the 8 × 8 pillar array outperformed the single pillar by a factor of 21.7. However, if contrasting the 2 × 2 and 8 × 8 arrays with the 24 μm² DOP region, the latter system demonstrated a 7.8 and 4.2 SERS response increase respectively.

Table S3. DOP Pitch Order Response Factor for arrays with a 520 nm pitch.

Array	Single DOP	2 × 2	4 × 4	8 × 8
2 × 2	11.7	—	—	—
4 × 4	18.1	1.6	—	—
8 × 8	21.7	1.9	1.2	—
24 μm ²	91.4	7.8	5.0	4.2

References

1. G. Lu, B. Shrestha, A.J. Haes. "Importance of Tilt Angles of Adsorbed Aromatic Molecules on Nanoparticle Rattle SERS Substrates". 2016. 120(37): 20759–20767. DOI: 10.1021/acs.jpcc.6b02023.
2. W. Gan, G. Gonella, M. Zhang, H.-L. Dai, et al. "Communication: Reactions and Adsorption at the Surface of Silver Nanoparticles Probed by Second Harmonic Generation". 2011. 134(4): 041104. doi: 10.1063/1.3548668.
3. S. Asiaei, P. Nieva, M.M. Vijayan. "Fast Kinetics of Thiolic Self-Assembled Monolayer Adsorption on Gold: Modeling and Confirmation by Protein Binding". J. Phys. Chem. B. 2014. 118(47): 13697–13703. doi: 10.1021/jp509986s.